AGU ADVANCING EARTH AND SPACE SCIENCE

Geophysical Research Letters

RESEARCH LETTER
10.1029/2020GL090420

Key Points:
- This study provided novel and detailed insights into the water-rock interactions following hydraulic fracturing
- Cation exchange, adsorption/desorption, and barite precipitation were observed both in the laboratory and field studies
- The oxidation of pyrite was not evident in field flowback samples that were dominated by mixing of fracturing fluids and formation water

Supporting Information:
- Supporting Information S1

Correspondence to:
T. Huang and B. Mayer,
tmhuang@mail.iggcas.ac.cn;
bmayer@ucalgary.ca

Citation:
Huang, T., Li, Z., Mayer, B., Nightingale, M., Li, X., Li, G., et al. (2020). Identification of geochemical processes during hydraulic fracturing of a shale gas reservoir: A controlled field and laboratory water-rock interaction experiment. *Geophysical Research Letters*, *47*, e2020GL090420. https://doi.org/10.1029/2020GL090420

Received 20 AUG 2020
Accepted 2 OCT 2020
Accepted article online 7 OCT 2020

Identification of Geochemical Processes During Hydraulic Fracturing of a Shale Gas Reservoir: A Controlled Field and Laboratory Water-Rock Interaction Experiment

Tianming Huang[1,2,3], Zhenbin Li[1,3], Bernhard Mayer[2], Michael Nightingale[2], Xiao Li[1,3], Guanfang Li[1,3], Yin Long[1,3], and Zhonghe Pang[1,3]

[1]Key Laboratory of Shale Gas and Geoengineering, Institute of Geology and Geophysics, Chinese Academy of Sciences, Beijing, China, [2]Department of Geoscience, University of Calgary, Calgary, Canada, [3]College of Earth and Planetary Sciences, University of Chinese Academy of Sciences, Beijing, China

Abstract A detailed study on geochemical processes following hydraulic fracturing can provide important information on the origin of solutes and potential improvement of fracturing technology. However, this remains difficult due to the low resolution of flowback water and high salinity of formation water. To fill this knowledge gap, a shale-gas well was drilled and freshwater was used to fracture the shale. In parallel, laboratory water-rock interaction experiments were conducted. The intensive sampling for flowback water and the use of multiple isotopes provided novel and detailed insights into the water-rock interactions after hydraulic fracturing. The results showed that beyond mixing processes, cation exchange, adsorption/desorption, and barite precipitation were observed both in the laboratory and field studies. Although oxidation of pyrite was observed in most of the laboratory experiments, our findings demonstrate that this process was not evident in field flowback samples that were dominated by mixing of fracturing fluids and formation water.

Plain Language Summary The hydraulic fracturing technologies have paved the way toward the development of unconventional shale gas from low-permeability shale reservoirs. The solutes in flowback water after hydraulic fracturing of shale gas reservoirs can originate from injected fracturing fluids and formation water, but may also be derived from solutes liberated by geochemical reactions. However, in most cases, the laboratory data do not match the field data from hydraulically fractured wells. To date, a further refined understanding of geochemical reactions after hydraulic fracturing occurred is critical for tracing the origin of solutes in flowback water (as the main potential pollutants for near-surface environments) and potentially improving the fracturing technology. Except for reported cation exchange and carbonate dissolution, this study showed several new findings, including nitrate adsorption/desorption and limited oxidation of pyrite in field flowback samples that were dominated by mixing of fracturing fluids and formation water, although oxidation of pyrite was observed in most of the laboratory experiments and expected to be comprehensive during field flowback after hydraulic fracturing. Therefore, the potential creation of matrix porosity induced by water-rock interactions of oxidation of pyrite and further induced dissolution of minerals may be limited.

1. Introduction

Horizontal drilling and high volume hydraulic fracturing technologies have paved the way toward the development of unconventional shale gas from low-permeability shale reservoirs over the last two decades (King, 2012). North America leads the world in the production of shale gas. In 2019, dry shale gas production in the United States totaled approximately 716 bcm, which was equal to approximately 75% of the total U.S. dry natural gas production in 2019 (EIA-U.S. Energy Information Administration, 2020). Fracturing fluids (water mixed with small amounts of sand and additives) are used to open existing and produce new fractures in the shale formation under high pressure to release natural gas. Previous studies showed that shale formation water (FOW) is immobile (Balashov et al., 2015; Engelder et al., 2014), and increases in the salinity of flowback water (FBW) are mainly caused by water-rock interactions (WRI) between fracturing fluids and shale (Balashov et al., 2015). However, increasing evidence has shown that FBW after hydraulic fracturing and produced water during the production of shale gas is a mixture of fracturing fluids and FOW, and FBW

at the late stage of flowback and produced water is mostly derived from FOW (e.g., Birkle, 2016; Haluszczak et al., 2013; Kondash et al., 2017). Because of the high salinity and the presence of toxic and radioactive compounds in FBW and produced water and possible leakage of gases, the potential threat to the shallow environment is of great concern (Brantley et al., 2018; Cahill et al., 2017; Lackey & Rajaram, 2019; Vengosh et al., 2014).

Although the mixing process between fracturing water (FRW) and FOW appears to be dominant for the water chemistry change of FBW, WRIs between water and shale may be expected to be significant in the early stage of flowback (e.g., Phan et al., 2018; Zolfaghari et al., 2016). The reactive minerals (e.g., pyrite, carbonates, organic matter, and clay) are widely distributed in most shale units (Heller & Zoback, 2014; Phan et al., 2020). A series of laboratory water and rock interaction experiments were conducted in the past to illustrate the geochemical processes following hydraulic fracturing (e.g., Harrison et al., 2017; Xu et al., 2018; Zeng et al., 2020). Geochemical processes observed in the laboratory included the oxidation of pyrite, dissolution of carbonates, and precipitation of specific minerals, including aluminosilicate (Herz-Thyhsen et al., 2019), Fe oxyhydroxide (Lu et al., 2017; Zolfaghari et al., 2016), and barite (Li et al., 2019; Paukert Vankeuren et al., 2017). These processes are also expected in the FBW of shale gas reservoirs (Zolfaghari et al., 2016).

However, in most cases, the laboratory data do not match the field data from hydraulically fractured wells (Phan et al., 2018; Zolfaghari et al., 2019) and sulfate concentrations of FBW are usually less explicable (Owen et al., 2020). This mismatch could be caused by (1) differences in the WRI conditions between the laboratory and field, such as different surface areas of reactive minerals or water/rock ratios (Harrison et al., 2017; Paukert Vankeuren et al., 2017); (2) additional additives (0.5–3.0 wt.%) in the fracturing fluid creating different reaction conditions (Wang et al., 2015); (3) failure to consider mixing of fracturing fluids and FOWs in addition to WRI (Zeng et al., 2020); (4) presence of organic species that are not always considered in the geochemical model database (Marcon et al., 2017); and (5) geologic heterogeneity (Phan et al., 2018). Also, previous research suggested that most WRI may occur at the very early stage of flowback and that mixing becomes increasingly dominant in controlling the chemical and isotopic composition in flowback at the late stage (Kondash et al., 2017). Therefore, daily sampling at the initial stage after hydraulic fracturing (Osselin et al., 2019; Phan et al., 2020) may not be sufficient for characterizing geochemical processes in detail. In addition, when the water chemistry of FBW is mainly controlled by the mixing process between FRW and FOW with very high salinity (tens to hundreds of g/L), the geochemical processes like cation exchanges and adsorption/desorption occurring at the very early stage of flowback may be masked. To date, a further refined understanding of geochemical reactions after hydraulic fracturing occurred is critical for tracing the origin of solutes in FBW (as the main potential pollutants for near-surface environments), improving the fracturing technology (Phan et al., 2020; Rosenblum et al., 2017), and extending knowledge of hydrogeochemical processes in deep low-permeability reservoirs.

In light of these limitations, this study aimed to characterize geochemical processes during hydraulic fracturing and flowback through (1) intensively sampling flowback fluids at the initial stage (hourly) at a field site after hydraulic fracturing, (2) simplifying the end-member of fracturing fluids in the field, and (3) using sulfur/nitrogen isotopes (for the first time) and other tracer techniques in laboratory and field experiments.

2. Material and Methods

2.1. Field Hydraulic Experiment

To facilitate the study of geochemical processes during hydraulic fracturing, a scientific vertical shale gas well (XK-3) with a depth of 704 m (supporting information Figure S1) was drilled into the Lower Silurian Longmaxi Marine Formation, Xishui, SW China, in 2019. The target stratum for the current commercial production of shale gas in the Sichuan Basin, SW China, is this formation. On 21 March 2019, FRW (500 m^3) was injected into the well with an injection rate of approximately 3 m^3/min under a pressure of 24–36 MPa to fracture the shale at a depth of 640–660 m without adding any additives on. This FRW was toxic and had a relatively low salinity with total dissolved solids (TDS) of 0.49 g/L and pH of 8.4. The freshwater was from a stream near the shale well. Before the fracturing, the water was collected in a water pond. After hydraulic fracturing, the flowback initiated on 24 March 2019. On the 1st day of flowback, the FBW was sampled approximately every 2 h and 10 FBW samples were collected. On the 2nd day, two additional samples were obtained. There was no flowback on the 3rd day because the well was shut in. From the 4th day to 26th day,

one or two FBW samples were collected each day. There was no flowback during the 27th–36th day. At the last stage of flowback, two samples of FBW on the 37th–38th day were collected (Table S1). The volume of cumulative water returned was 267 m^3. There were one fresh FRW sample and 38 FBW samples in total. One rock core of the shale at the fracturing depth was also sampled after drilling was completed.

2.2. Laboratory Water-Rock Experiment

In parallel, laboratory WRI experiments were conducted to verify data trends observed in the field data and identify the underlying WRI processes. The original porosity of the shale core is 4.2%. The shale core sample (at the fracturing depth) was crushed using a disc mill (Disc Mill DM 200) and sieved using a sieve shaker with sieve mesh number of 200. As a result, the shale powder with the grain size lower than 74 μm was obtained. Each rock sample was placed into a 50 ml centrifuge tube, and then deionized water or FRW was added with a water/rock ratio of 2 (i.e., 30 ml of water and 15 g of shale) for all the experiments, although the water/rock ratio during field fracturing is highly variable (Paukert Vankeuren et al., 2017; Renock et al., 2016). These tubes were placed into a water bath with a temperature of 28°C (reservoir temperature at the fracturing depth) and then shaken for 2 min to 7 days. For different measurement purposes (e.g., S, O, N, and C isotope ratios), several sets of WRI experiments were conducted under the same conditions. After the reaction, the tubes were centrifuged at 4,500 rpm for 15 min. The supernatant solution was filtered through 0.45 μm filters. A nitrate desorption experiment was also conducted using deionized water and 2 mol/L KCl solution. The pressure was not considered in the WRI experiments because (1) during hydraulic fracturing and subsequent flowback, the changes in pressure are quite dynamic (Birdsell et al., 2015; Edwards & Celia, 2018; McIntosh & Ferguson, 2019) and (2) the impact of pressure on most wetness parameters is limited (Harrison et al., 2017; Morel & Hering, 1993; Zolfaghari et al., 2019). The cation exchange capacity (CEC) of the shale sample was measured by using the sodium acetate method strictly following U.S. EPA Method 9081.

2.3. Analyses

The description of analyses of chemical (Cl, SO_4, F, Ca, Mg, Na, K, NO_3, NH_4, NO_2, Br, B, Sr, Li, Ba, Fe, Mn, and other trace elements) and isotopic composition (δ^2H-H_2O, δ^{18}O-H_2O, δ^{34}S-SO_4, δ^{18}O-SO_4, δ^{15}N-NO_3, δ^{18}O-NO_3, δ^{15}N-NH_4, δ^{13}C-DIC, ^{3}H, and ^{14}C-DIC) for FRW, FBW, and water samples from laboratory WRI experiment was introduced in detail in supporting information. Saturation indices of mineral phases were calculated using PHREEQC software based on the PHREEQC.DAT database (Parkhurst & Appelo, 1999).

3. Results and Discussion

3.1. Hydraulic Fracturing Field Experiment

The fresh FRW had a relatively low salinity with concentrations of TDS of 0.49 g/L, Cl of 12.5 mg/L, Br of 0.03 mg/L, SO_4 of 158 mg/L, NO_3 of 15.9 mg/L, Na of 36 mg/L, Ca of 104 mg/L, Mg of 8.2 mg/L, Ba of 0.064 mg/L, B of 0.07 mg/L, and NH_4 concentrations below the detection limit (<0.04 mg/L) (Table S1). The saturation indices of calcite and barite were 1.07 and 0.26, suggesting supersaturation. After hydraulic fracturing, the flowback started and the TDS, Cl, and Br concentrations increased initially rapidly and subsequently in a more moderate fashion (Figure 1). Meanwhile, the ^{14}C-DIC and ^{3}H contents of FBW decreased. On the 37th day and 38th day, the ^{14}C content was 6.3 and 5.5 pMC, respectively, and FBW contained no ^{3}H (<0.4 TU). This suggests that the FBW on the 37th–38th day was paleowater and was likely tens of thousands of years old compared with the ^{14}C content of 93.3 pMC and ^{3}H content of 9.8 TU of FRW (Table S1; Figure 1) representing modern (since the 1950s) recharged water. The ^{3}H and ^{14}C results suggest that the FBW at the end stage was not derived from FRW, but from local FOW.

At the end of flowback (i.e., on the 37th–38th day), the FBW had TDS concentration of 11.50–11.92 g/L, Cl of 4,342–4,411 mg/L, SO_4 of 10–11 mg/L (with δ^{34}S-SO_4 of 36.4–44.7‰ and δ^{18}O-SO_4 of 21.5–22.7‰), NO_3 of 14.0–14.3 mg/L, Ba of 4.33–5.18 mg/L, B of 5.88–5.91 mg/L, and NH_4 of 12.84–13.60 mg/L (Table S1). If the FBW at the end of flowback is taken as an end-member FOW, then the mixing ratios can be estimated based on the two end-members (FRW and FOW) using Cl as a conservation tracer (Osselin et al., 2018; Warner et al., 2014). Figure 1 shows that the fraction of FOW steadily increased to 50% on the 4th day and 80% after 2 weeks. When 500 m^3 FRW was injected into the well, 267 m^3 was returned, of which 115 m^3 was derived from FRW and 152 m^3 was from FOW based on the chloride mass balance (Figure S2).

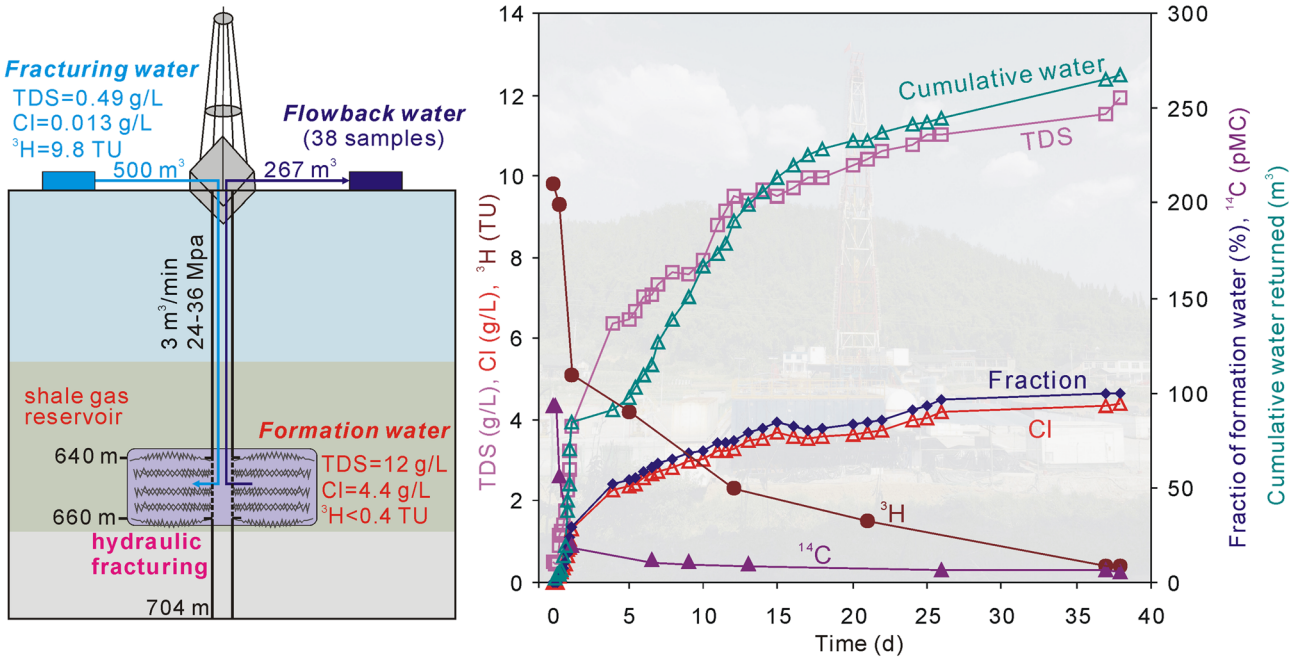

Figure 1. The conceptual model of the field experiment and changes in the contents of the main chemical indicators (total dissolved solids (TDS) and Cl) and isotopes (^{14}C and ^{3}H) during flowback. The volume of water recovered with flowback time has also been shown (267 m^3 of water was finally returned). At the end stage of flowback, no ^{3}H was detected and the ^{14}C concentration was as low as 5.5–6.3 pMC, thereby suggesting that these flowback waters were not derived from the fracturing water but local formation water.

The calculated mixing fraction can be used to determine whether there are other geochemical processes in the low-permeability reservoir affecting the chemical and isotopic compositions of FBW beyond mixing between FRW and local FOW. The results showed that the observed SO_4 concentrations and $\delta^{34}S$-SO_4 in the FBW plotted close to the mixing line (Figures 2g and 2h). However, the Na concentration increased (Figure 2a) while the Ca and Mg concentrations decreased (Figures 2b and 2c) beyond mixing trends in the first 10 days, especially during 10–26 h of flowback (Table S2). The HCO_3 concentration showed an increasing trend in the first week beyond what was expected from mixing alone (Figure 2d). There was a linear negative relationship (R^2 of 0.84) between the increase in Na + K concentration and decrease in Ca + Mg concentration (Figure 2f). There was also an increasing trend in NH_4 and B concentrations beyond mixing (Figures 2j and 2l). Meanwhile, the NO_3 concentrations sharply decreased from 15.9 mg/L in FRW to 0.1–1.0 mg/L in the FBW in the first half-day of flowback, and subsequently NO_3 concentrations gradually increased from 1.4 to 14.3 mg/L (Figure 2k).

3.2. Laboratory WRI Experiment

Laboratory analyses revealed that the shale sample from the hydraulically fractured formation was composed of quartz (39.3%), plagioclase (6.6%), carbonate (10.1%; 9.6% for calcite and 0.5% for dolomite), pyrite (3.8%), and clay (40.2%). The total organic content was 3.4%. The CEC of the shale sample was 54 meq/kg. The $\delta^{34}S$ values for soluble sulfate, acid volatile sulfides, and chromium reducible sulfides (mainly pyrite) were 4.3‰, 9.0‰, and −5.1‰, respectively. However, S in the shale sample occurred predominantly as pyrite while soluble sulfate represented less than 2% of total S. The ^{13}C value of carbonates in the shale samples was 0.0‰.

The laboratory WRI experiment with deionized water and shale with a ratio of 2 at 28°C from 2 min to 7 days showed that SO_4 (65–68%) and HCO_3 (26–31%) were the major anions and Na (59–71%) and K (20–23%) were the major cations in all water samples (Table S3). No NO_3 was detected (<0.1 mg/L). With increasing WRI time (from 2 min to 7 days), there were generally increasing trends in the concentrations of SO_4, Na, K, Ca, Mg, and B and a decreasing trend in the concentration of Ba. The concentrations of Cl (average of 18 mg/L) and NH_4 (average of 4.3 mg/L) remained constant with increasing WRI time (Table S3). Through analyzing sulfur and carbon isotopes, oxidation of pyrite, dissolution of carbonate, cation exchange between Ca + Mg and Na + K, and barite precipitation (Figure 3) were observed during the laboratory WRIs

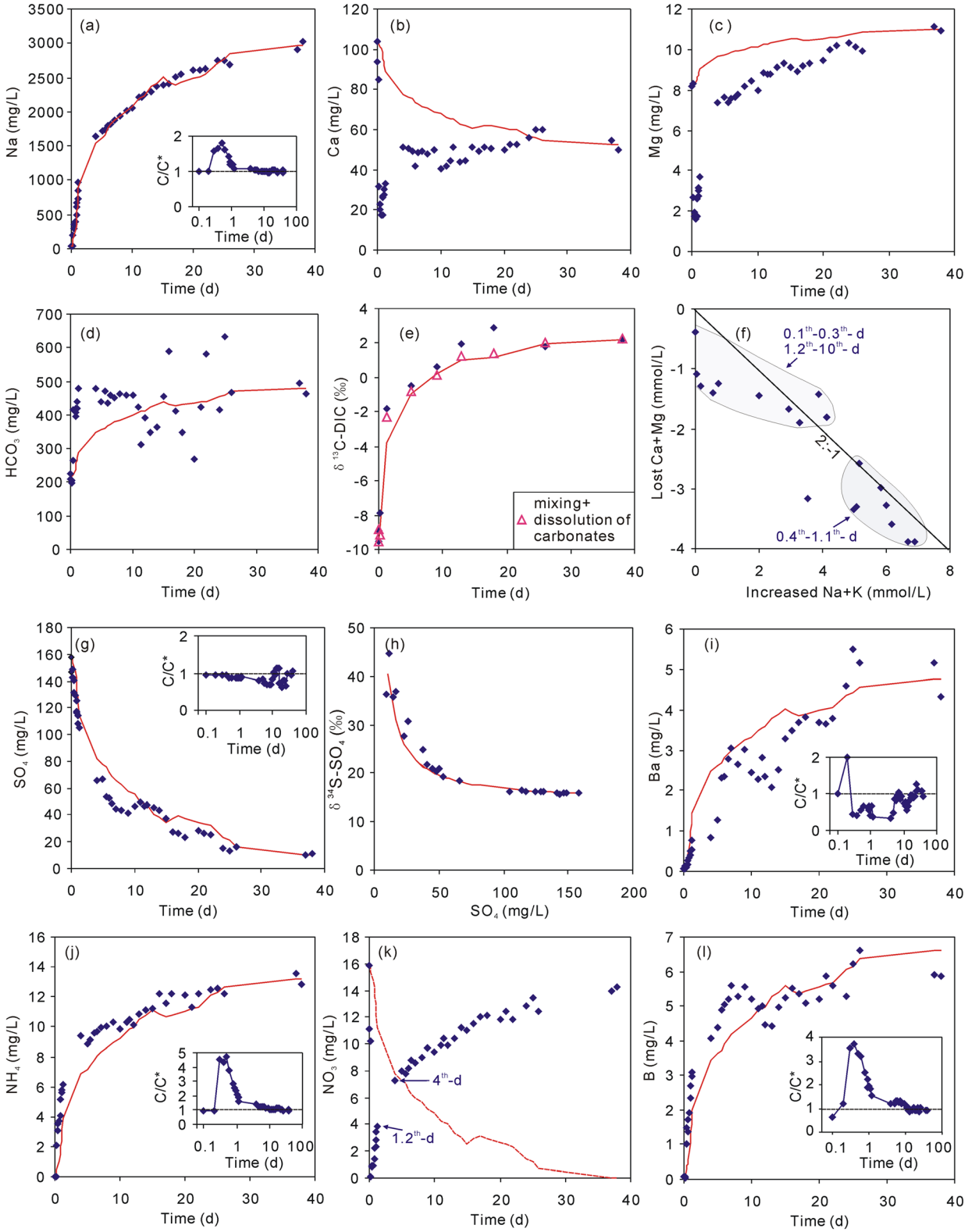

Figure 2. Geochemical and isotopic evolution for specific ions. The red line represents the mixing between the fracturing water (FRW) and formation water (FOW) using Cl as a tracer and the blue diamond represents the observed value. C^* = concentration derived from the mixing process; C = observed concentration. The evolution of Na, Ca, Mg, HCO_3, δ^{13}C-DIC, SO_4, Ba, NH_4, NO_3, and B concentration with flowback time is shown in panels a, b, c, d, e, g, i, j, k, and h, respectively. The relationship between the amount of lost Ca+Mg and increased Na+K is shown in panel f. The relationship between the δ^{34}S-SO_4 value and SO_4 concentration is shown in panel h.

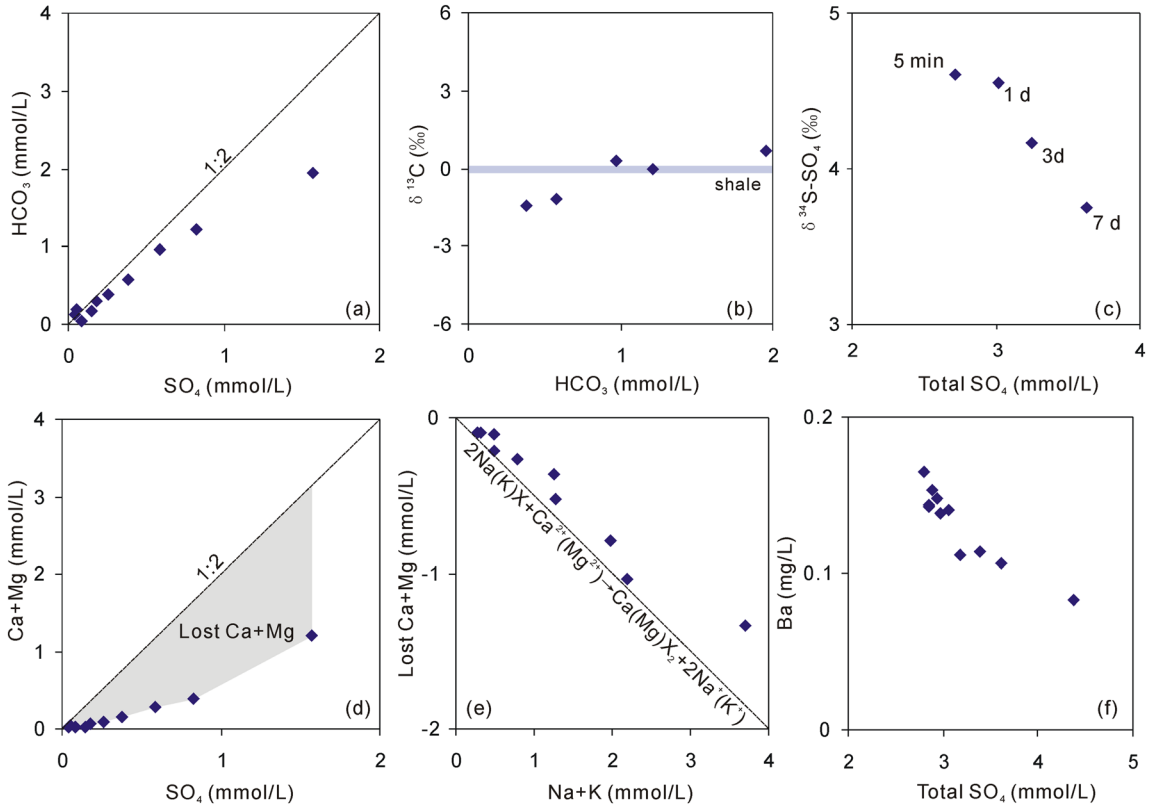

Figure 3. The evolution of selected ions and isotopes during water-rock interaction between deionized water and shale. Based on the process of the oxidation of pyrite and further dissolution of carbonates (Equation S1), the mole ratio of SO_4:HCO_3 was close to 1:2 (a) and HCO_3 was mainly derived from the dissolution of carbonates. The $\delta^{13}C$ value of dissolved inorganic carbon (mainly as HCO_3 with a pH of 7.5–8.2) matched the $\delta^{13}C$ value for the shale rock (0.0‰) (b). The oxidation of pyrite decreased the $\delta^{34}S$-SO_4 value but increased total SO_4 concentration (c). The decreases in the Ca + Mg concentration (lost Ca + Mg) during the water-rock interaction (d) were related to the Na + K concentrations (e), thereby suggesting that cation exchange occurred between Ca + Mg and Na + K. The increase in the SO_4 concentration led to oversaturation and then precipitation of barite, thereby resulting in a decrease in the Ba concentration (f).

experiments (supporting information). There was no precipitation of carbonates during the WRI and the impact of barite precipitation on the SO_4 concentration was very limited (<0.14 mg/L).

When the shale samples were reacted with FRW, the concentration of Ca decreased from 106 to 24–26 mg/L, that of Mg decreased from 8.1 to 4.9–5.2 mg/L, and that of NO_3 decreased from 14.3 to 4.0–4.1 mg/L in the first 5 min (Table S4). Meanwhile, the Na concentration increased from 38 to 226–235 mg/L, that of K increased from 4.0 to 108–112 mg/L, and that of SO_4 increased from 153 to 364–370 mg/L (Table S4). The overall trends for Ca, Mg, Na, K, and NO_3 were similar to those of the field data in the early stage of flowback (Figure 2). The evolution characteristics of these ions (Figure S3) were similar to those of the WRI between deionized water and shale (Figure 3), thereby suggesting that reactions responsible for the observed trends included the oxidation of pyrite, dissolution of carbonates, cation exchange, and barite precipitation.

However, the NO_3 concentration did not further change significantly (from 3.7 to 4.9 mg/L) and was unrelated to the WRI time (Figure S4). The FRW and water samples from the WRI had similar $\delta^{15}N$-NO_3 (9.2–9.5‰) and $\delta^{18}O$-NO_3 (1.2–3.7‰) values (Figure S4). Deionized water and KCl solution were then used to continue to extract any retained NO_3 in the remaining shale samples in four successive extractions (Table S5). The results showed that the desorption experiment can recover 66% of the NO_3 in the original FRW using deionized water and 89% using the KCl solution.

3.3. Discussion

Previous studies have shown that in the first month of flowback, the FBW is a mixture of FRW and FOW and the late FOW is dominant in FBW (Birkle, 2016; Warner et al., 2014). Our study shows that FOW accounted

for 50% of the FBW on the 4th day and 80% after 2 weeks (Figure 1). This is comparable with other cases; e.g., in a hydraulically fractured horizontal well in a low-permeability reservoir within the Marcellus Formation in the United States showed that the fraction of the FOW in the FBW increased from 5–8% on the 1st day to 50% after 12th day (Warner et al., 2014). A similar case in the Qusaiba Hot Shale in Saudi Arabia showed that the FOW was 28% on the 4th day of flowback but was 100% after 40th day (Birkle, 2016). Based on the mass balance, approximately 43% of returned FBW (i.e., 115 m^3) was derived from FRW and 57% from FOW (i.e., 152 m^3). However, the salinity was mainly derived from FOW (e.g., 99.8% chloride in FBW was from FOW).

Owing to the intensive sampling conducted during the initial flowback period (10 samples on the 1st day), we were able to determine that cation exchange reactions are occurring between Ca + Mg and Na + K with a negative relationship (Figure 2f), which was also confirmed by the WRI experiments and measurement of the CEC. The sharp decrease in the Ca concentration from 100 to 17.4 mg/L in the FBW cannot be explained by the precipitation of calcite because the SI of calcite for FBW (0.02–1.02 with an average value of 0.56 in the first week) was always lower than that of FRW (1.07). The increase in HCO_3 concentration beyond mixing suggested that the dissolution of carbonates occurred, as confirmed by the δ^{13}C-DIC values (Figures 2d and 2e). Therefore, it is concluded that carbonate is dissolved increasing Ca concentrations but ion exchange immediately retains this Ca and releases Na in solution. Although the phenomenon and theory are not new concepts, this study has clearly shown the comprehensive cation exchange at the early stage of flowback compared to previous studies. The cation exchange in the field was rarely reported in previous studies due to relatively sparse sampling (i.e., low resolution data) and high salinity of the FOW from industry wells (tens to hundreds of g/L compared to ~12 g/L in this study), which could mask the cation exchange due to mixing process between FRW and FOW.

There was an increasing trend in B concentrations beyond mixing for FBW (Figure 2l), which was caused by the desorption from clays (Phan et al., 2020; Warner et al., 2014). In the WRI experiments, B concentrations showed an increasing trend with increasing WRI time (Tables S3 and S4). Field experiment showed additional NH_4 was observed in FBW beyond mixing (Figure 2j), which was released from shale and confirmed from the laboratory experiments (average concentration of 4.3 mg/L for NH_4 in water samples with deionized water/rock ratio of 2). The effect of barite precipitation had a negligible impact on SO_4 concentrations (Figure 2g) (supporting information). One of the most interesting trends during initial flowback was the decrease in NO_3 concentration from 15.4 mg/L in FRW to 0.1 mg/L after 7 h of flowback (at this stage, FRW still accounted for 97%). This was also observed in the laboratory WRI experiment (Figure S4; Table S4), i.e., from 14.3 to 4.0–4.1 mg/L in 5 min. This decrease in NO_3 concentration was not caused by denitrification but absorption (Figure S5; supporting information).

The decrease in the concentration and increase in the δ^{34}S value of SO_4 during flowback can be mathematically explained as the reduction in SO_4 in FRW. However, FBW samples do not plot perfectly on a Rayleigh fractionation trend for sulfate reduction (process a, b, and c in Figure 4) with S isotope enrichment factors ranging from −60‰ to −9‰ (Krouse & Mayer, 2000; Mayer et al., 2007). Because O_2 is present in FRW and atmospheric O_2 is entrained in the injected FRW (Xu et al., 2018; Zolfaghari et al., 2016) and other oxidizers (such as a persulfate breaker or H_2O_2) are added to fracturing fluids at shale gas sites (Osselin et al., 2019; Phan et al., 2020), and because there are always pyrite minerals in shales (Heller & Zoback, 2014), oxidation of pyrites after hydraulic fracturing and during initial flowback is very likely (Osselin et al., 2019; Paukert Vankeuren et al., 2017; Xu et al., 2018; Zolfaghari et al., 2016). Laboratory experiments have revealed evidence for oxidation of pyrites (Pearce et al., 2018; Xu et al., 2018; d and e in Figure 4), which would contribute additional SO_4 to the FBW. However, in our field experiment, even an additional 10 mg/L of SO_4 derived from the oxidation of pyrite in the shale at the initial stage of flowback (158 + 10 mg/L) would deviate from the mixing line (g in Figure 4), suggesting that the data did not provide evidence for pyrite oxidation. Even in industrial practices, when a strong oxidizer (persulfate breaker) is used during hydraulic fracturing, SO_4 derived from pyrite oxidation was found to be negligible (<4 mg/L) based on S isotope analyses (Osselin et al., 2019). Although the availability of O_2 was not limiting for the pyrite oxidation in most laboratory experiments including our laboratory experiments, this may not be the case at the field scale owing to the highly reducing conditions in shale gas reservoirs and the high rock to O_2 ratio (Balashov et al., 2015; Harrison et al., 2017). In the measurements of produced water from two wells of

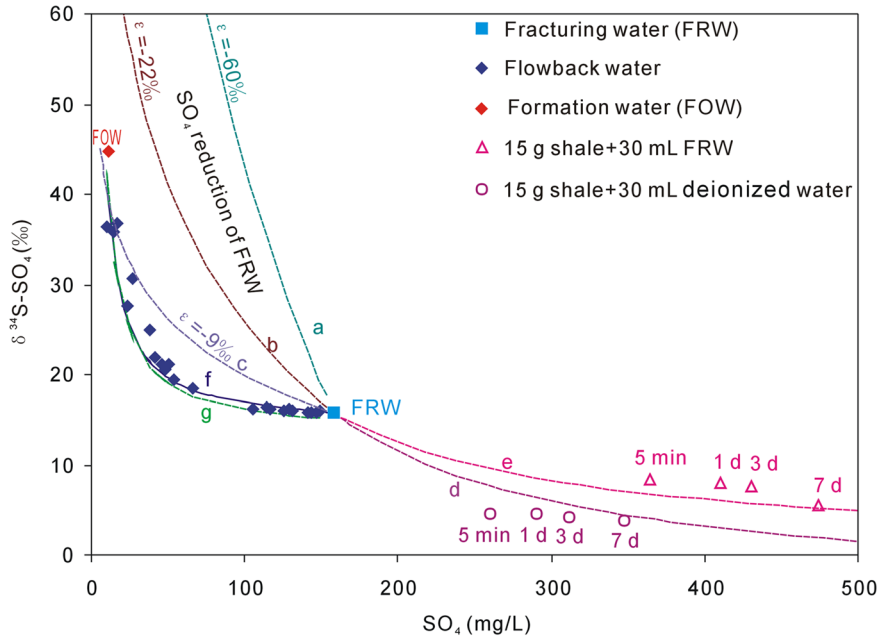

Figure 4. The plot of the S isotopes of SO_4 (δ^{34}S-SO_4) against the SO_4 concentrations. (a, b, and c) The lines for SO_4 reduction of fracturing water with enrichment factors of −60‰ and −9‰ as the lower and upper reported values and −22‰ as the typical value, respectively. (d and e) Lines for the SO_4 of fracturing water mixed with SO_4 derived from the oxidation of pyrite in the shale with an δ^{34}S value of −5.1‰ and mixed with SO_4 derived from any S in the shale with an δ^{34}S value of −0.1‰ (derived from a 9-day WRI between deionized water and shale, the 3rd set of laboratory water-rock interaction in Table S3), respectively. (f) Mixing line between fracturing water and formation water. (g) Line for fracturing water first mixed with the SO_4 derived from the shale (additional 10 mg/L is assumed) and then mixed with formation water.

the Marcellus Shale (both anhydrite and gypsum were not detected), SO_4 was undetected and S concentration was approximately 3 mg/L in the produced water on day 1 and day 2 (Phan et al., 2020), which was assumed to be attributed to the removal of S during the fracturing period by either adsorption of ammonium persulfate on shale minerals or precipitation of SO_4 derived from persulfate oxidation as gypsum or barite. The low sulfate concentrations after production times of more than 2 months were also assumed to be attributed to bacterial SO_4 reduction under a more reducing environment in the reservoir (Engle & Rowan, 2014; Phan et al., 2020). However, because FBW was undersaturated with respect to gypsum (saturation indices of ≤1.3) in our study and the effect of precipitation of $BaSO_4$ on the SO_4 concentration was shown to be very limited, precipitation of SO_4 minerals was not a major factor influencing sulfate concentration. Our chemical and isotopic data for field samples revealed that FBW plotted on a mixing line between FRW and FOW (f in Figure 4; also for the plot of δ^{34}S against δ^{18}O in Figure S6). This suggests that neither oxidation of pyrite nor reduction of SO_4 were important processes impacting the chemical composition of FRW.

4. Conclusions and Implications

The intensive sampling with a high resolution during the initial stage of flowback (within 1 day) from a shallow hydraulically fractured well designed for scientific research made it possible to determine the geochemical processes during WRI in considerable detail. Within the 2 days of flowback, cation exchange and nitrate absorption had a considerable impact on the cation and NO_3 concentrations. These complex geochemical reactions in the very early stage of flowback (such as cation exchange and adsorption/desorption) modify the ion ratios (e.g., Na/Cl, Ca/Na, and B/Cl), which have been commonly used to trace the origin of water and solutes. Therefore, care should be taken when the ion ratios are used in early stage of flowback. However, after 2 days of flowback, the chemical composition of FBW is dominated by mixing. Oxidation of pyrite in field hydraulic fracturing and flowback, which was expected, is not evident.

This study will help to improve our understanding of the geochemical processes during hydraulic fracturing of low-permeability hydrocarbon reservoirs and help to identify and trace the origin of specific pollutants related to the exploration and production of shale gas plays. Beyond the reported WRIs (e.g., cation exchange and adsorption/desorption), this study found that further dissolution of minerals (especially carbonates) and potential creation of matrix porosity induced by the oxidation of pyrite (Harrison et al., 2017; Okamoto et al., 2017) may be limited. When the mixing of FOW and FRW appears to dominate the overall water quality evolution of FBW, the WRI during hydraulic fracturing and flowback seems not to pose an important environmental issue if leaked.

Data Availability Statement

Data can be found in the Global Change Research Data Publishing and Repository (GCdataPR) at http://www.geodoi.ac.cn/WebEn/doi.aspx?Id=1586.

Acknowledgments

This study was supported by the National Natural Science Foundation of China (grant 41877207), the Strategic Priority Research Program (B) of the Chinese Academy of Sciences (grant XDB10030603), the Science Foundation of Key Laboratory of Shale Gas, and Geoengineering of the Chinese Academy of Sciences (grant KLSG201708), IAEA Project (grant RAS7035), the Youth Innovation Promotion Association CAS (grant 2018087), and a CAS scholarship (grant 201825). We thank Baoqiang Ma and Jiao Tian for their help during field sampling; Steve Taylor, Jesusa Pontoy, Veith Becker, and Yiman Li for help in isotopes and water chemistry measurement; and Pauline Humez, Chunfang Cai, Xiaorong Luo, Jianming He, Yibo Wang, Jaime Cesar, and Jiao Tian for helpful discussion.

References

Balashov, V. N., Engelder, T., Gu, X., Fantle, M. S., & Brantley, S. L. (2015). A model describing flowback chemistry changes with time after Marcellus Shale hydraulic fracturing. *AAPG Bulletin*, *99*(01), 143–154. https://doi.org/10.1306/06041413119

Birdsell, D. T., Rajaram, H., Dempsey, D., & Viswanathan, H. S. (2015). Hydraulic fracturing fluid migration in the subsurface: A review and expanded modeling results. *Water Resources Research*, *51*, 7159–7188. https://doi.org/10.1002/2015WR017810

Birkle, P. (2016). Geochemical fingerprinting of hydraulic fracturing fluids from Qusaiba Hot Shale and formation water from Paleozoic petroleum systems, Saudi Arabia. *Geofluids*, *16*(3), 565–584. https://doi.org/10.1111/gfl.12176

Brantley, S. L., Vidic, R. D., Brasier, K., Yoxtheimer, D., Pollak, J., Wilderman, C., & Wen, T. (2018). Engaging over data on fracking and water quality. *Science*, *359*(6374), 395–397. https://doi.org/10.1126/science.aan6520

Cahill, A. G., Steelman, C. M., Forde, O., Kuloyo, O., Ruff, S. E., Mayer, B., et al. (2017). Mobility and persistence of methane in groundwater in a controlled-release field experiment. *Nature Geoscience*, *10*(4), 289–294. https://doi.org/10.1038/ngeo2919

Edwards, R. W. J., & Celia, M. A. (2018). Shale gas well, hydraulic fracturing, and formation data to support modeling of gas and water flow in shale formations. *Water Resources Research*, *54*, 3196–3206. https://doi.org/10.1002/2017WR022130

EIA-U.S. Energy Information Administration (2020). Energy Information Administration. Annual Energy Outlook 2020. https://www.eia.gov

Engelder, T., Cathles, L. M., & Bryndzia, L. T. (2014). The fate of residual treatment water in gas shale. *Journal of Unconventional Oil and Gas Resources*, *7*, 33–48. https://doi.org/10.1016/j.juogr.2014.03.002

Engle, M. A., & Rowan, E. L. (2014). Geochemical evolution of produced waters from hydraulic fracturing of the Marcellus Shale, northern Appalachian Basin: A multivariate compositional data analysis approach. *International Journal of Coal Geology*, *126*, 45–56. https://doi.org/10.1016/j.coal.2013.11.010

Haluszczak, L. O., Rose, A. W., & Kump, L. R. (2013). Geochemical evaluation of flowback brine from Marcellus gas wells in Pennsylvania, USA. *Applied Geochemistry*, *28*, 55–61. https://doi.org/10.1016/j.apgeochem.2012.10.002

Harrison, A. L., Jew, A. D., Dustin, M. K., Thomas, D. L., Joe-Wong, C. M., Bargar, J. R., et al. (2017). Element release and reaction-induced porosity alteration during shale-hydraulic fracturing fluid interactions. *Applied Geochemistry*, *82*, 47–62. https://doi.org/10.1016/j.apgeochem.2017.05.001

Heller, R., & Zoback, M. (2014). Adsorption of methane and carbon dioxide on gas shale and pure mineral samples. *Journal of Unconventional Oil and Gas Resources*, *8*, 14–24. https://doi.org/10.1016/j.juogr.2014.06.001

Herz-Thyhsen, R. J., Kaszuba, J. P., & Dewey, J. C. (2019). Dissolution of minerals and precipitation of an aluminosilicate phase during experimentally simulated hydraulic fracturing of a mudstone and a tight sandstone in the Powder River Basin, WY. *Energy & Fuels*, *33*(5), 3947–3956. https://doi.org/10.1021/acs.energyfuels.8b04443

King, G. E. (2012). Hydraulic fracturing: What every representative, environmentalist, regulator, reporter, investor, university researcher, neighbor and engineer should know about estimating frac risk and improving frac performance in unconventional gas and oil wells. Paper presented at SPE 152596, SPE Hydraulic Fracturing Technology Conference, Woodlands, Texas, USA. https://doi.org/10.2118/152596-MS

Kondash, A. J., Albright, E., & Vengosh, A. (2017). Quantity of flowback and produced waters from unconventional oil and gas exploration. *Science of the Total Environment*, *574*, 314–321. https://doi.org/10.1016/j.scitotenv.2016.09.069

Krouse, H. R., & Mayer, B. (2000). Sulphur and oxygen isotopes in sulphate. In P. G. Cook & A. L. Herczeg (Eds.), *Environmental tracers in subsurface hydrology* (pp. 195–231). Boston: Kluwer Academic Publishers. https://doi.org/10.1007/978-1-4615-4557-6_7

Lackey, G., & Rajaram, H. (2019). Modeling gas migration, sustained casing pressure, and surface casing vent flow in onshore oil and gas wells. *Water Resources Research*, *55*, 298–323. https://doi.org/10.1029/2018WR024066

Li, Q., Jew, A. D., Kohli, A., Maher, K., Brown, G. E. Jr., & Bargar, J. R. (2019). Thicknesses of chemically altered zones in shale matrices resulting from interactions with hydraulic fracturing fluid. *Energy & Fuels*, *33*(8), 6878–6889. https://doi.org/10.1021/acs.energyfuels.8b04527

Lu, J., Mickler, P. J., Nicot, J. P., Choi, W., Esch, W. L., & Darvari, R. (2017). Geochemical interactions of shale and brine in autoclave experiments—Understanding mineral reactions during hydraulic fracturing of Marcellus and Eagle Ford Shales. *AAPG Bulletin*, *101*(10), 1567–1597. https://doi.org/10.1306/11101616026

Marcon, V., Joseph, C., Carter, K. E., Hedges, S. W., Lopano, C. L., Guthrie, G. D., & Hakala, J. A. (2017). Experimental insights into geochemical changes in hydraulically fractured Marcellus Shale. *Applied Geochemistry*, *76*, 36–50. https://doi.org/10.1016/j.apgeochem.2016.11.005

Mayer, B., Alpay, S., Gould, W. D., Lortie, L., & Rosa, F. (2007). The onset of anthropogenic activity recorded in lake sediments in the vicinity of the Horne smelter in Quebec, Canada: Sulfur isotope evidence. *Applied Geochemistry*, *22*(2), 397–414. https://doi.org/10.1016/j.apgeochem.2006.10.001

McIntosh, J. C., & Ferguson, G. (2019). Conventional oil—The forgotten part of the water-energy nexus. *Groundwater*, *57*(5), 669–677. https://doi.org/10.1111/gwat.12917

Morel, F. M. M., & Hering, J. G. (1993). *Principles and applications of aquatic chemistry* (p. 608). New York: Wiley-Interscience.

Okamoto, A., Tanaka, H., Watanabe, N., Saishu, H., & Tsuchiya, N. (2017). Fluid pocket generation in response to heterogeneous reactivity of a rock fracture under hydrothermal conditions. *Geophysical Research Letters*, *44*, 10,306–10,315. https://doi.org/10.1002/2017GL075476

Osselin, F., Nightingale, M., Hearn, G., Kloppmann, W., Gaucher, E., Clarkson, C. R., & Mayer, B. (2018). Quantifying the extent of flowback of hydraulic fracturing fluids using chemical and isotopic tracer approaches. *Applied Geochemistry*, *93*, 20–29. https://doi.org/10.1016/j.apgeochem.2018.03.008

Osselin, F., Saad, S., Nightingale, M., Hearn, G., Desaulty, A. M., Gaucher, E. C., et al. (2019). Geochemical and sulfate isotopic evolution of flowback and produced waters reveals water-rock interactions following hydraulic fracturing of a tight hydrocarbon reservoir. *Science of the Total Environment*, *687*, 1389–1400. https://doi.org/10.1016/j.scitotenv.2019.07.066

Owen, J., Bustin, R. M., & Bustin, A. M. M. (2020). Insights from mixing calculations and geochemical modeling of Montney Formation post hydraulic fracturing flowback water chemistry. *Journal of Petroleum Science and Engineering*, *195*, 107589. https://doi.org/10.1016/j.petrol.2020.107589

Parkhurst, D. L., & Appelo, C. A. J. (1999). *User's Guide to PHREEQC (Version 2): A compute program for speciation, batch-reaction, one-dimensional transport, and inverse geochemical calculations* (p. 312). Denver, CO: U.S. Geological Survey.

Paukert Vankeuren, A. N., Hakala, J. A., Jarvis, K., & Moore, J. E. (2017). Mineral reactions in shale gas reservoirs: Barite scale formation from reusing produced water as hydraulic fracturing fluid. *Environmental Science & Technology*, *51*(16), 9391–9402. https://doi.org/10.1021/acs.est.7b01979

Pearce, J. K., Turner, L., & Pandey, D. (2018). Experimental and predicted geochemical shale water reactions: Roseneath and Murteree shales of the Cooper Basin. *International Journal of Coal Geology*, *187*, 30–44. https://doi.org/10.1016/j.coal.2017.12.008

Phan, T. T., Hakala, J. A., & Sharma, S. (2020). Application of isotopic and geochemical signals in unconventional oil and gas reservoir produced waters toward characterizing in situ geochemical fluid-shale reactions. *Science of the Total Environment*, *714*, 136867. https://doi.org/10.1016/j.scitotenv.2020.136867

Phan, T. T., Paukert Vankeuren, A. N., & Hakala, J. A. (2018). Role of water-rock interaction in the geochemical evolution of Marcellus Shale produced waters. *International Journal of Coal Geology*, *191*, 95–111. https://doi.org/10.1016/j.coal.2018.02.014

Renock, D., Landis, J. D., & Sharma, M. (2016). Reductive weathering of black shale and release of barium during hydraulic fracturing. *Applied Geochemistry*, *65*, 73–86. https://doi.org/10.1016/j.apgeochem.2015.11.001

Rosenblum, J., Nelson, A. W., Ruyle, B., Schultz, M. K., Ryan, J. N., & Linden, K. G. (2017). Temporal characterization of flowback and produced water quality from a hydraulically fractured oil and gas well. *Science of the Total Environment*, *596–597*, 369–377. https://doi.org/10.1016/j.scitotenv.2017.03.294

Vengosh, A., Jackson, R. B., Warner, N., Darrah, T. H., & Kondash, A. (2014). A critical review of the risks to water resources from unconventional shale gas development and hydraulic fracturing in the United States. *Environmental Science & Technology*, *48*(15), 8334–8348. https://doi.org/10.1021/es405118y

Wang, L., Fortner, J. D., & Giammar, D. E. (2015). Impact of water chemistry on element mobilization from Eagle Ford Shale. *Environmental Engineering Science*, *32*(4), 310–320. https://doi.org/10.1089/ees.2014.0342

Warner, N. R., Darrah, T. H., Jackson, R. B., Millot, R., Kloppmann, W., & Vengosh, A. (2014). New tracers identify hydraulic fracturing fluids and accidental releases from oil and gas operations. *Environmental Science & Technology*, *48*(21), 12,552–12,560. https://doi.org/10.1021/es5032135

Xu, M., Binazadeh, M., Zolfaghari, A., & Dehghanpour, H. (2018). Effects of dissolved oxygen on water imbibition in gas shales. *Energy & Fuels*, *32*(4), 4695–4704. https://doi.org/10.1021/acs.energyfuels.7b03955

Zeng, L., Reid, N., Lu, Y., Hossain, M. M., Saeedi, A., & Xie, Q. (2020). Effect of the fluid–shale interaction on salinity: Implications for high-salinity flowback water during hydraulic fracturing in shales. *Energy & Fuels*, *34*(3), 3031–3040. https://doi.org/10.1021/acs.energyfuels.9b04311

Zolfaghari, A., Dehghanpour, H., & Bearinger, D. (2019). Produced flowback salts vs. induced-fracture interface: A field and laboratory study. *SPE Journal*, *24*(03), 1309–1321. https://doi.org/10.2118/185078-PA

Zolfaghari, A., Dehghanpour, H., Noel, M., & Bearinger, D. (2016). Laboratory and field analysis of flowback water from gas shales. *Journal of Unconventional Oil and Gas Resources*, *14*, 113–127. https://doi.org/10.1016/j.juogr.2016.03.004

References From the Supporting Information

Ali, M., & Hascakir, B. (2017). Water/rock interaction for Eagle Ford, Marcellus, Green River, and Barnett Shale samples and implications for hydraulic-fracturing-fluid engineering. *SPE Journal*, *22*(01), 162–171. SPE-177304-PA. https://doi.org/10.2118/177304-PA

Davies, R. J., Mathias, S. A., Moss, J., Hustoft, S., & Newport, L. (2012). Hydraulic fractures: How far can they go? *Marine and Petroleum Geology*, *37*(1), 1–6. https://doi.org/10.1016/j.marpetgeo.2012.04.001

Flewelling, S. A., Tymchak, M. P., & Warpinski, N. (2013). Hydraulic fracture height limits and fault interactions in tight oil and gas formations. *Geophysical Research Letters*, *40*, 3602–3606. https://doi.org/10.1002/grl.50707

Groffman, P. M., Altabet, M. A., Böhlke, J. K., Butterbach-Bahl, K., David, M. B., Firestone, M. K., et al. (2006). Methods for measuring denitrification: Diverse approaches to a difficult problem. *Ecological Applications*, *16*(6), 2091–2122. https://doi.org/10.1890/1051-0761(2006)016[2091:MFMDDA]2.0.CO;2

Kendall, C., & Aravena, R. (2000). Nitrate isotopes in groundwater systems. In P. G. Cook & A. L. Herczeg (Eds.), *Environmental tracers in subsurface hydrology* (pp. 1–80). Boston: Kluwer Academic Publishers. https://doi.org/10.1007/978-1-4615-4557-6_9

Mayer, B., & Krouse, H. R. (2004). Procedures for sulfur isotope abundance studies. In P. A. de Groot (Ed.), *Handbook of stable isotope analytical techniques* (Vol. 1, pp. 538–596). New York: Elsevier. https://doi.org/10.1016/B978-044451114-0/50028-4

Sebilo, M., Mayer, B., Grably, M., Billiou, D., & Mariotti, A. (2004). The use of the ammonium diffusion' method for δ^{15}N-NH_4^+ and δ^{15}N-NO_3^- measurements: Comparison with other techniques. *Environmental Chemistry*, *1*(2), 99–103. https://doi.org/10.1071/EN04037

Sigman, D. M., Casciotti, K. L., Andreani, M., Barford, C., Galanter, M., & Böhlke, J. K. (2001). A bacterial method for the nitrogen isotopic analysis of nitrate in seawater and freshwater. *Analytical Chemistry*, *73*(17), 4145–4153. https://doi.org/10.1021/ac010088e

Welch, S. A., & Ullman, J. (1996). Feldspar dissolution in acidic and organic solutions: Compositional and pH dependence of dissolution rate. *Geochimica et Cosmochimica Acta*, *60*(16), 2939–2948. https://doi.org/10.1016/0016-7037(96)00134-2

Zhao, H., Ma, F., Liu, G., & Feng, X. (2017). Numerical study of hydraulic fracturing in heterogeneous rocks under different hydraulic loading conditions. *Journal of Engineering Geology*, *25*, 1328–1335. https://doi.org/10.13544/j.cnki.jeg.2017.05.020